0026-895X/09/7504-812–819$20.00
MOLECULAR PHARMACOLOGY
Copyright © 2009 The American Society for Pharmacology and Experimental Therapeutics
Mol Pharmacol 75:812–819, 2009

Vol. 75, No. 4
52605/3454042
Printed in U.S.A.

A Small-Molecule Triptolide Suppresses Angiogenesis and Invasion of Human Anaplastic Thyroid Carcinoma Cells via Down-Regulation of the Nuclear Factor-κB Pathway[S]

Wenbo Zhu, Yanqiu Ou, Yan Li, Ru Xiao, Minfeng Shu, Yuehan Zhou, Jun Xie, Songmin He, Pengxin Qiu, and Guangmei Yan

Department of Pharmacology, Zhong-shan Medical College, Sun Yat-Sen University, Guangzhou, People's Republic of China

Received October 9, 2008; accepted January 21, 2009

ABSTRACT

Anaplastic thyroid carcinoma (ATC) is among the most aggressive malignancies known and is characterized with rapid growth, early invasion, and complete refractoriness to current therapies. Here we report that triptolide, a small molecule from a Chinese herb, could potently inhibit proliferation in vitro, angiogenesis in vivo, and invasion in a Matrigel model in human ATC cell line TA-K cells at nanomolar concentrations. We further elucidate that triptolide inhibits the nuclear factor-κB (NF-κB) transcriptional activity via blocking the association of p65 subunit with CREB-binding protein (CBP)/p300 in the early stage and via decreasing the protein level of p65 in the late stage. Expression of the NF-κB targeting genes cyclin D1, vascular endothelial growth factor, and urokinase-type plasminogen activator is significantly reduced by triptolide in both TA-K and 8505C human ATC cell lines, which are well known to be critical for proliferation, angiogenesis, and invasion in solid tumors. Our findings suggest that triptolide may function as a small molecule inhibitor of tumor angiogenesis and invasion and may provide novel mechanistic insights into the potential therapy for human ATC.

Anaplastic thyroid carcinoma (ATC) is one of the most rapidly growing and invasive types of thyroid malignancies and is probably the most destructive cancer encountered in humans (Neff et al., 2008). Although it represents only 2 to 5% of all thyroid cancers, ATC accounts for approximately more than half of thyroid carcinoma deaths (McIver et al., 2001). Despite multimodal therapy, including surgery, chemotherapy, and radiotherapy, this tumor has a dismal prognosis, with a mean survival of 3 to 4 months after diagnosis (Pasieka, 2003). Thus, novel treatment strategies are urgently needed to ameliorate the lethality of this malignancy.

Angiogenesis and invasion are characteristic features of malignant neoplasms and play prominent roles in the progression of cancer (Carmeliet and Jain, 2000; Mareel and Leroy, 2003). ATC displays pathologic angiogenesis that leads directly to the rapid growth of masses. Meanwhile, in ATC in particular, tumor cells invade outward into neighboring organs, such as trachea and esophagus, in a high percentage of patients, causing rapid death (Neff et al., 2008). Many molecular events may be involved in the angiogenesis and invasion of solid malignant tumors, including ATC, but recent intensive researches have focused on the key role of vascular endothelial growth factor (VEGF) (Hicklin and Ellis, 2005). VEGF has been well established to be not only a major mediator of angiogenesis via regulating majority steps in the angiogenic cascades, but also a promoter of invasion via directly disrupting endothelial barrier function (Ferrara et al., 2003; Schmitt et al., 2004; Weis et al., 2004). In fact, targeting VEGF by macromolecules such as monoclonal antibodies against VEGF or VEGF receptor constitutes an attractive therapy (Prewett et al., 1999; Ferrara et al., 2005). It is noteworthy that the endogenous level of VEGF is controlled by multiple important machineries, among which the NF-κB pathway is a pivotal one (Chilov et al., 1997). Therefore, it seems reasonable to hypothesize that targeting the NF-κB pathway, by macromolecules or small molecules, may provide a novel therapeutic modality for cancers with significant angiogenesis and invasion (ATC, for instance).

This work was supported by Key Program, National Natural Science Foundation of China [Grant 30830111] and National Natural Science Foundation of China [Grant 330801408].

W.Z., Y.O., and Y.L. contributed equally to this work.

Article, publication date, and citation information can be found at http://molpharm.aspetjournals.org.

doi:10.1124/mol.108.052605.

[S] The online version of this article (available at http://molpharm.aspetjournals.org) contains supplemental material.

ABBREVIATIONS: ATC, anaplastic thyroid carcinoma; VEGF, vascular endothelial growth factor; IκB, inhibitor of κB; NF-κB, nuclear factor κB; MTT, 3-(4,5-dimethylthiazol-2-yl)-2,5-diphenyl tetrazolium bromide; uPA, urokinase-type plasminogen activator; ELISA, enzyme-linked immunosorbent assay; PCR, polymerase chain reaction; CBP, cAMP response element-binding protein binding protein.

Triptolide is a small (M_r 360) and easily synthesized diterpenoid triepoxide originally purified from the Chinese herb *Tripterygium wilfordii* Hook.f (Supplemental Fig. 1). It has well documented activity for the treatment of rheumatoid arthritis as a result of its anti-inflammatory and immunosuppressive effects (Chen, 2001). In addition, triptolide has been reported to inhibit proliferation and induce apoptosis of cancer cells in vitro and reduce the growth and metastases of tumors in vivo (Chang et al., 2001; Yang et al., 2003). However, the effects of triptolide on tumor angiogenesis and invasion remain unknown.

In the present study, we show that triptolide is capable of suppressing proliferation in vitro, angiogenesis in vivo, and invasion in a Matrigel model in human TA-K ATC cells at an extremely low dose. These effects have been associated with the inhibition of NF-κB targeting genes, which results from the suppressed interaction of p65 subunit of NF-κB with CBP/p300 and the decreased p65 protein.

Materials and Methods

Cell Culture and Drug Treatment. Human ATC cell line TA-K cells were kindly provided by Dr. Hui Sun (Jilin University, Changchun, Jilin, People's Republic of China) and maintained in William's medium E (Invitrogen, Carlsbad, CA) , supplemented with 10% fetal bovine serum. Another ATC cell line, 8505C (European Collection of Cell Cultures, Wiltshire, UK), was maintained in Dulbecco's modified Eagle's medium (Invitrogen), supplemented with 10% new-born calf serum. Cells were cultured in a 5% CO2–humidified atmosphere at 37°C. Triptolide (Sigma-Aldrich, St. Louis, MO) was dissolved in dimethyl sulfoxide to obtain a 1 mM stock solution and stored at 4°C. for drug treatment, triptolide was diluted in medium and added as indicated concentrations for indicated time.

Cell Viability and Proliferation Assay. The viability of cells was determined by the 3-(4,5-dimethylthiazol-2-yl)-2,5-diphenyl tetrazolium bromide (MTT; Sigma) assay. In brief, cells were seeded in 96-well plates at 2×10^3 cells/well and incubated overnight. After different treatment for various times, 20 μl of MTT solution (5 mg/ml in phosphate-buffered saline) was added to each well to induce the production of formazan crystals. MTT solution was aspired off after 4 h, and 100 μl of DMSO was added to achieve solubilization of the formazan crystal. The optical density (OD) was determined at 570 nm using an EXL800 microimmunoanalyser (Bio-Tek Instruments, Burlington, VT).

For cell proliferation assay, a 5-bromo-2′-deoxyuridine (BrdU) cell proliferation ELISA kit (Roche Diagnostics, Mumbai, India) was used according to the manufacturer's instructions. Cells seeded in 96-well plates at 2×10^3 cells/well were labeled with BrdU for 4 h then anti-BrdU-POD Fab fragments and substrate were added in sequence. The OD was determined at 405 nm using an EXL800 microimmunoanalyzer. Results were normalized to the cell number.

Caspase 3 Activity Assay and Hoechst Staining. Caspase 3 enzymatic activity was evaluated using caspase 3 activity assay kit (Roche Diagnostics). After different treatment for various times, cells was resuspended in 100 μl of lysate at a concentration of 2×10^6 cells/ml. After spallation, lysate was incubated with anti-caspase 3 coating solution and blocking buffer in sequence. Then, a 100-μl sample was transferred to microplate well. After incubation, samples were removed and substrate solution was added. The microplate was incubated for 3 h at 37°C in the dark. The OD was determined at 400 nm using an EXL800 microimmunoanalyzer. For Hoechst 33258 staining, cells were fixed with 4% paraform for 10 min, stained with Hoechst 33258 (5 μg/ml; Sigma) for 15 min in the dark, and observed by fluorescence microscopy (Olympus, Melvile, NY) with a 340-nm excitation filter.

Matrigel Angiogenesis Assay. The angiogenesis on Matrigel was measured as described previously (Fang et al., 2007). In brief, aliquots of cells (0.2 ml, 1×10^7 cells/ml) were mixed with 0.4 ml of 10 mg/ml growth factor-reduced Matrigel (R&D Systems, Minneapolis, MN) in the presence or absence of 30 nM triptolide. The mixture was immediately injected into both flanks of BALB/C-nu nude mice (female, 4 weeks old; purchased from Experimental Animal Center of Southern Medical University, Guangzhou, China). Ten days later, the Matrigel plugs were removed from the mice and photographed. Hemoglobin levels of Matrigel plugs were quantified with Drabkin's reagent (Sigma).

Cell Invasion Assay. Cell invasion was assayed in a cell culture chamber (BD Biosciences Discovery Labware, Bedford, MA) with 8-μm pore size polycarbonate membrane filters. The filters were precoated with 50 μl of Matrigel (1.25 mg/ml). Cells treated with triptolide for 12 or 24 h were harvested and seeded in upper chambers at a density of 10^5 cells/well with serum-free medium. Meanwhile, 0.6 ml of complete medium with 10% fetal bovine serum and 20 ng/ml VEGF165 (Peprotech Asia, Rehovot, Israel) was placed in bottom chambers. At the same time, moreover, equal cells of the second group (treated and untreated) were plated to 96-well plates for cell number assay (MTT). The chamber was incubated at 37°C for 24 h and then the Matrigel was removed with a cotton bud. The invaded cells were fixed with 4% paraform, stained with hematoxylin, photographed, and counted. The invasiveness of TA-K cells was determined by the percentage-of-invasion score (invaded cell number/total cell number × 100%).

Western Blot, Immunoprecipitation, and ELISA Analysis. Western blot was carried out as described previously (Qiu et al., 1999). The following antibodies were used: VEGF neutralizing antibody (10 μg/ml; R&D Systems), antibodies against β-actin (1:1000; Thermo Scientific IHC, Fremont, CA), tubulin (1:5000; Sigma), IκBα, phosphorylated-IκBα (1:1000; BD Biosciences, San Jose, CA), p65, uPA (1:200; Santa Cruz Biotechnology, Santa Cruz, CA), cyclin D1, and p65-Ser276, 468, 536 (1:1000; Cell Signaling Technology, Danvers, MA) .

Immunoprecipitation was conducted as described previously (Lee et al., 1999). Cellular protein was immunoprecipitated with a CBP mouse antibody (2 μg/10^6 cells; BD Biosciences) followed by Western blot analysis with a p65 mouse antibody (1:1000; Santa Cruz Biotechnology). Tubulin was used as loading control and nonspecific IgG (6 μg/10^6 cells; Upstate Biotechnology Inc., Lake Placid, NY) was used as negative control.

VEGF concentration was determined using a VEGF ELISA kit (R&D Systems) according to the manufacturer's instructions. The culture medium was collected, centrifuged to remove cellular debris, and stored at −70°C until assay for VEGF. Results were normalized to the cell number.

EMSA and Luciferase Activity. DNA binding of NF-κB was detected by EMSA. Nuclear proteins were extracted using Nuclear and Cytoplasmic Extraction Reagents (Pierce, Rockford, IL). An oligonucleotide corresponding to the NF-κB binding site consensus sequence (5′-AGTTGAGGGGACTTTCCCAGGC-3′) was synthesized and end-labeled with biotin by Invitrogen (Jiang et al., 2001). Electrophoretic mobility shift assay reaction mixtures contained 10 μg of nuclear protein extract, and 1 pmol of probes were incubated at room temperature for 20 min, run on a 4% polyacrylamide gel, transferred to nylon membrane, and cross-linked for 1 min. Then the nylon membrane was detected using a Chemiluminescent Nucleic Acid Detection Module (Pierce). C23 (also designated nucleolin; 1:500; Santa Cruz Biotechnology), was used as a protein loading control.

For luciferase activity assays, TA-K cells were cotransfected with 60 ng of NF-κB luciferase reporter plasmid (Stratagene, La Jolla, CA) and 60 ng of *Renilla reniformis* luciferase reporter vector pGL-3 (Promega, Madison, WI) per well using Lipofectamine 2000 (Invitrogene) for 24 h. Cells were treated with triptolide for further 12 h and harvested for analysis of luciferase activity using the dual luciferase reporter assay system (Promega). Luminence was measured by Glo-

Max 96 Microplate Luminometer with dual injectors (Promega). The firefly luciferase luminescence activity was normalized to the control *R. reniformis* luciferase activity.

Reverse Transcription-Polymerase Chain Reaction. Total RNA was reverse transcribed using Superscript II reverse transcriptase (Invitrogen), cDNA was used for PCR and the primer sequences were as follows: cyclin D1, 5′-CCCTCGGTGTCCTACTTCAAA-3′ (sense) and 5′-CACCTCCTCCTCCTCCTCTTC-3′ (antisense); uPA, 5′-TAAGAGCTGGTGTCTGATTG-3′ (sense) and 5′-TTGGATGAACTAGGCTAAAA-3′ (antisense); VEGF, 5′-TCGGGCCTCCGAAACCATGA-3′ (sense) and 5′-CCTGGTGAGAGATCTGGTTC-3′ (antisense); and glyceraldehyde-3-phosphate dehydrogenase, 5′-CCACCCATGGCAAATTCCATGGCA-3′ (sense) and 5′-TCTAGACGGCAGGTCAGGTCCACC-3′ (antisense). The PCR conditions contained an initial cDNA synthesis reaction at 48°C for 1 h, followed by a denaturation step for 2 min at 94°C and 30 cycles: 1 min at 94°C, 1 min at 55°C, and 1 min at 72°C. After the last cycle, the final extension was performed at 72°C for 10 min. PCR products were analyzed by agarose gel electrophoresis and visualized with ethidium bromide staining.

Statistical Analysis. Data are presented as mean ± S.D. of three separate experiments. Statistical significance was determined by Student's *t* test. *P* values <0.05 were considered statistically significant.

Results

Triptolide Inhibited Proliferation and Induced Apoptosis of Human TA-K ATC Cells. Triptolide has been shown to inhibit proliferation and induce apoptosis in multiple human cancer cell lines (Chan et al., 2001; Kiviharju et al., 2002). To test whether triptolide also has the same effects in ATC cells, cell viability was firstly analyzed by MTT assay. As seen in Fig. 1A, the TA-K cell viability dropped to its minimum at 30 nM within 48 h of triptolide exposure, and the mean concentration inducing a 50% of maximal inhibitory effect (IC_{50}) was calculated to be 67 nM. In addition, the inhibitory effect of triptolide (30 nM) on cell viability was time-dependent from 24 to 96 h (Fig. 1B). Triptolide is clearly able to cause the loss of cell viability in ATC cells.

BrdU incorporation assay was further performed to determine cell proliferation. As seen in Fig. 1C, a time-dependent reduction of cell proliferation was observed with triptolide treatment from 24 to 48 h; at 48 h, the cell proliferation decreased by 29.5%.

Caspase 3 enzymatic activity analysis and Hoechst staining were used to investigate whether the treatment of trip-

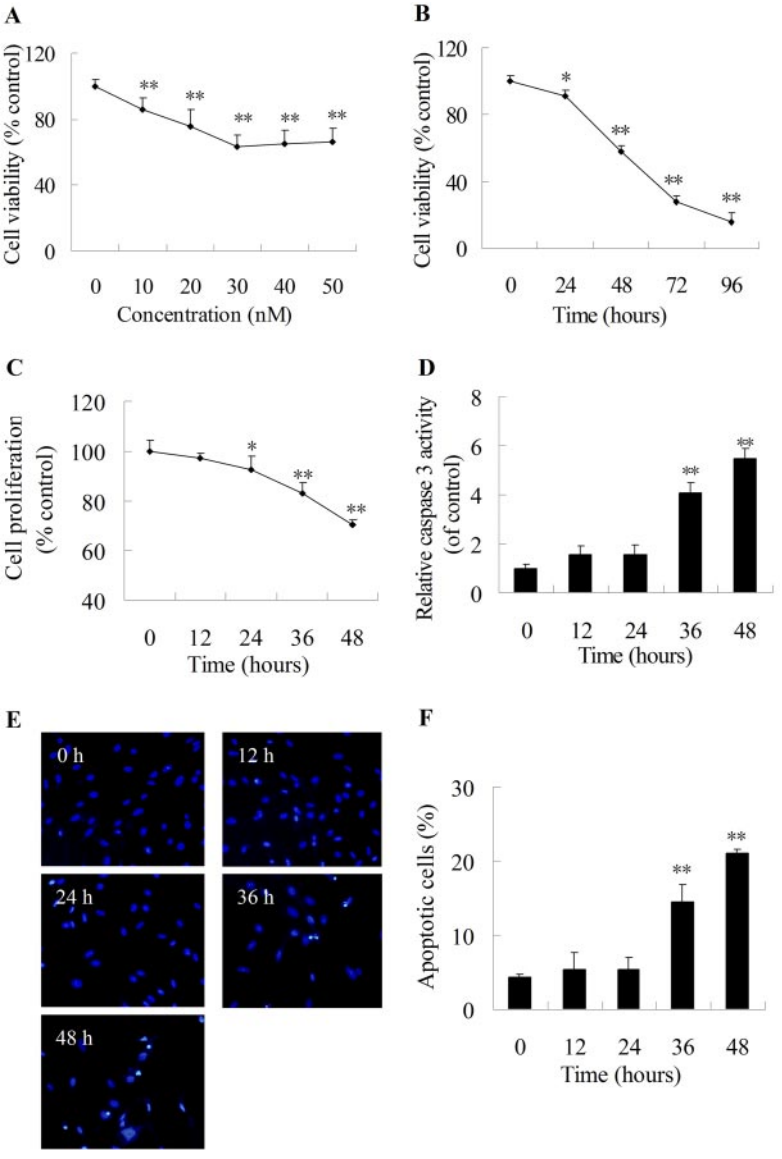

Fig. 1. Triptolide inhibited proliferation and induced apoptosis of human TA-K ATC cells. A, the concentration-dependent effect of triptolide on the cell viability. TA-K cells were treated with 0, 10, 20, 30, 40, and 50 nM triptolide for 48 h. B–E, TA-K cells were incubated with 30 nM triptolide for the indicated time. B, the time-dependent effect of triptolide on the cell viability. C, the time-dependent effect of triptolide on cell proliferation. D, the time-dependent effect of triptolide on caspase 3 activity. E, Hoechst 33258 staining on TA-K cells. F, the quantitation of the percentage of apoptotic cells. The data are mean ± S.D. ($n = 3$). *, $p < 0.05$, **, $p < 0.01$ compared with the control.

tolide caused apoptosis. Caspase 3 activity markedly enhanced after 36-h triptolide treatment, and apoptotic cells with characteristic morphological alterations such as condensed nuclei and cell shrinkage were observed (Fig. 1, D–F). Hence, the reduction of cell viability seems to be caused, at least in part, by decreased proliferation within the time course of 24 h, and apoptosis may also contribute to this reduction after 36 h.

Triptolide Reduced Tumor Neovascularization in Vivo. Given the crucial role of neovascularization in ATC, we next examined the possible effect of triptolide on angiogenesis in vivo. Angiogenic properties of tumor cells can be assayed using a Matrigel system (Fang et al., 2007). Figure 2A showed that TA-K cells induced formation of blood vessels in the Matrigel plug. The addition of triptolide significantly inhibited the tumor cell-induced angiogenesis at a concentration of 30 nM. Matrigel alone had no effect on angiogenesis. To further quantify the relative angiogenesis in plugs, hemoglobin contents were determined. Compared with control, triptolide decreased hemoglobin levels by approximately 60% ($p < 0.01$; Fig. 2B). This result indicates that triptolide has the potent capability to inhibit ATC tumor neovascularization.

Triptolide Suppressed Invasion of TA-K Cells. Invasiveness is an important factor for the prognosis of patients with ATC. We thus tested whether triptolide may also affect the invasiveness of TA-K cells. Matrigel invasion analysis confirmed that triptolide led to a remarkable reduction of invading cells in a dose-dependent manner with a maximal suppression effect at 30 nM (Fig. 3A). Triptolide has also displayed a strong inhibitory effect on cell invasion in a time-dependent manner (Fig. 3B). As seen in Fig. 3B, triptolide (30 nM) diminished the invasion ability of the TA-K cells to 8.1% of the controls at 24 h ($p < 0.01$). In addition, we examined cell death by lactate dehydrogenase release assay and observed that obvious cell death occurred after 36-h treatment (Supplemental Fig. 2), making sure that the invasion experiment was performed before massive cell death.

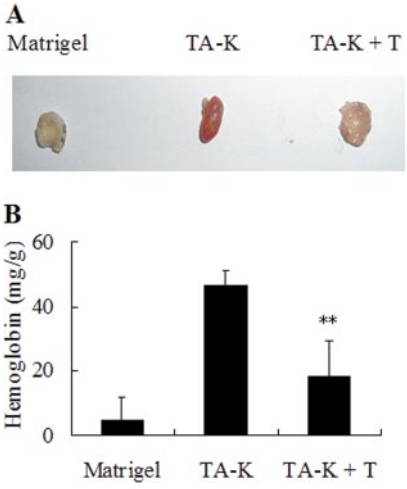

Fig. 2. Triptolide repressed tumor neovascularization in vivo. Aliquots of TA-K cells were mixed with Matrigel in the presence or absence of triptolide (T), injected into nude mice and removed 10 days later. A, angiogenesis in Matrigel plugs. B, hemoglobin levels of Matrigel plugs. Hemoglobin was quantified with Drabkin's reagent. The data are mean ± S.D. ($n = 5$). *, $p < 0.05$; **, $p < 0.01$ compared with the control.

Thus, the results of Matrigel-based invasion assay indicate that triptolide can regulate the invasion of cancer cells.

Triptolide Decreased NF-κB Transcriptional Activity by Blocking Association of p65 Subunit with CBP/p300 and Decreasing the Protein Level of p65. To understand the molecular mechanisms by which triptolide suppresses angiogenesis and invasion, we examined the NF-κB transcriptional activity of human ATC. As seen in Fig. 4A, triptolide significantly inhibited the NF-κB activity in a dose-dependent manner at 12 h with a luciferase reporter assay. It reached its maximal effect at 30 nM. To elucidate the exact mechanism of inhibited NF-κB transcriptional activity by triptolide in the early stage, we investigated a number of regulatory factors important for NF-κB signaling within 12 h of triptolide exposure. First, the level of NF-κB's inhibitory protein IκBα was examined. The total and phosphorylated IκBα remained steady (Fig. 4B). It is noteworthy that after longer exposure, as one of NF-κB target genes, IκBα protein began to decline in a time-dependent manner (data not shown), giving rise to a negative feedback loop (Hoffmann et al., 2002). Then, the DNA binding of NF-κB was analyzed. As indicated in Fig. 4C, no marked change was observed in three concentration groups tested. Next, we focused on the three specific serine residues of p65 Ser276, Ser468, and Ser536 that contribute to NF-κB transactivation activity (Zhong et al., 1998; Mattioli et al., 2006) and observed no significant alteration (Fig. 4D). Finally, considering that the binding of p65 to transcriptional coactivator CBP/p300 is required for NF-κB transactivation (Zhong et al., 2002), we examined the association of p65 and CBP/p300. Immunoprecipitation analysis showed significant blockage on the binding of p65 to CBP/p300 (Fig. 4E). All together, these data suggested that triptolide inhibits NF-κB transcriptional activity at least in part by blocking the association of p65 with CBP/p300.

We then probed the effect of triptolide on NF-κB protein level upon extended exposure. We noticed that p65, the active component of NF-κB, remained stable for 24 h and then began dramatically dropping (Fig. 4F). These results suggest that triptolide may also affect p65 stability. The dual action of triptolide on the interaction of p65/CBP and p65 stability may account for its drastic effect on the down-regulation of the NF-κB function.

Triptolide Down-Regulated Expression of NF-κB Downstream Genes in TA-K Cells. NF-κB is constitutively active in most tumor cell lines and regulates a series of genes involved in cell growth, angiogenesis, and invasion, such as cell cycle regulatory gene cyclin D1, pro-invasion gene uPA, and angiogenesis-promoting factor VEGF (Aggarwal, 2004; Karin, 2006). We thus examined the consequence of triptolide's suppression of NF-κB by monitoring the expression of these NF-κB targeting genes. Figure 5A showed that VEGF mRNA began to decrease at 12 h after triptolide exposure, whereas the mRNA levels of cyclin D1 and uPA markedly reduced at 36 h. Western blot and ELISA analysis also revealed significantly decreased protein levels of cyclin D1, uPA (Fig. 5B), and VEGF (Fig. 5C) in triptolide-treated cells, which are consistent with the effect on transcriptional activity (Fig. 5A). Besides, all of three protein levels were decreased in a concentration-dependent manner (Supplemental Fig. 3 and Fig. 5D). It is possible that VEGF may be reduced in response to the earlier NF-κB activity inhibition,

whereas cyclin D1 and uPA may decline after p65 protein reduction.

Triptolide Repressed NF-κB Activity, p65 Expression, and Its Downstream Genes in Human 8505C ATC Cell Line. To test whether the effects of triptolide in TA-K cells is cell-specific or not, another human ATC cell line 8505C cells were used. After exposure to triptolide as low as 30 nM for 12 h, NF-κB transcriptional activity displayed the same alteration panel as in TA-K cells (Fig. 6A). However, the decreasing of p65 protein was observed at 24 h after treatment, earlier than in TA-K cells (Fig. 6B). Down-regulation of cyclin D1, uPA, and VEGF in response to triptolide was also seen in 8505C cells as in TA-K cells (Fig. 6, C–E). These findings demonstrate that triptolide may have a broad therapeutic potential in ATC.

Discussion

ATC has been a real challenge for its rapid growth, early invasion, dimmed therapies, and high mortality. Seventy-six percent of patients with ATC in diagnosis have a rapidly enlarging neck mass that results from excessive and pathological angiogenesis. And patients with a tumor larger than 6.0 cm occasionally live less than 12 months (Tan et al., 1995). McIver et al. (2001) demonstrated that 98% local invasion is present in patients with ATC (McIver et al., 2001). Nevertheless, few treatments could save or even extend lives of patients with ATC, and researches on ATC are countable. These realities demand the urgent development of effective therapeutic options, such as agents for restricting tumor angiogenesis and invasion. Here we demonstrated that triptolide, a well known antirheumatoid arthritis agent, significantly inhibits proliferation, angiogenesis, and invasion of human TA-K ATC cells, suggesting a potential antineoplastic effect of this small molecule in ATC. Triptolide may offer a much needed therapeutic strategy for patients with ATC.

To effectively use triptolide for clinical development, it is essential to understand its mode of actions and potential biomarkers. Accumulating evidence suggests that inhibition of NF-κB could repress tumor angiogenesis, invasion, and tumorigenicity through down-regulating its downstream genes expression (Huang et al., 2000; Huang et al., 2001; Kong et al., 2007). Our work demonstrates that triptolide could inhibit NF-κB transcriptional activity, consistent with most of previous studies (Lee et al., 1999; Jiang et al., 2001). It is noteworthy that DNA binding of NF-κB was not affected simultaneously. NF-κB consisting of a heterotrimer of p50 and p65 binds to its inhibitory protein IκBα in an inactive form in the cytoplasm. The phosphorylation, ubiquitination, and degradation of IκBα led to the release of the p50-p65 heterodimer, which then translocates to the nucleus and associates with the promoter regions of multiple target genes (Baldwin, 1996). Phosphorylation of p65 at specific serine residues, such as Ser276, Ser468, and Ser536 enhances NF-κB transactivation activity (Zhong et al., 1998; Mattioli et al., 2006), and the interaction of p65 with transcriptional coactivator CBP/p300 is indispensable for NF-κB transactivation (Zhong et al., 2002). We further elucidate here that the NF-κB inhibition is due in part to the blockage of the association of p65 subunit with the transcriptional coactivator CBP/p300 (i.e., a precise mechanism for transactivation inhibition). In addition, we discovered that triptolide was able to decrease p65 protein level as well further potentiating the inhibition of NF-κB activity. These effects lead to down-regulation of a number of NF-κB targeting genes, including

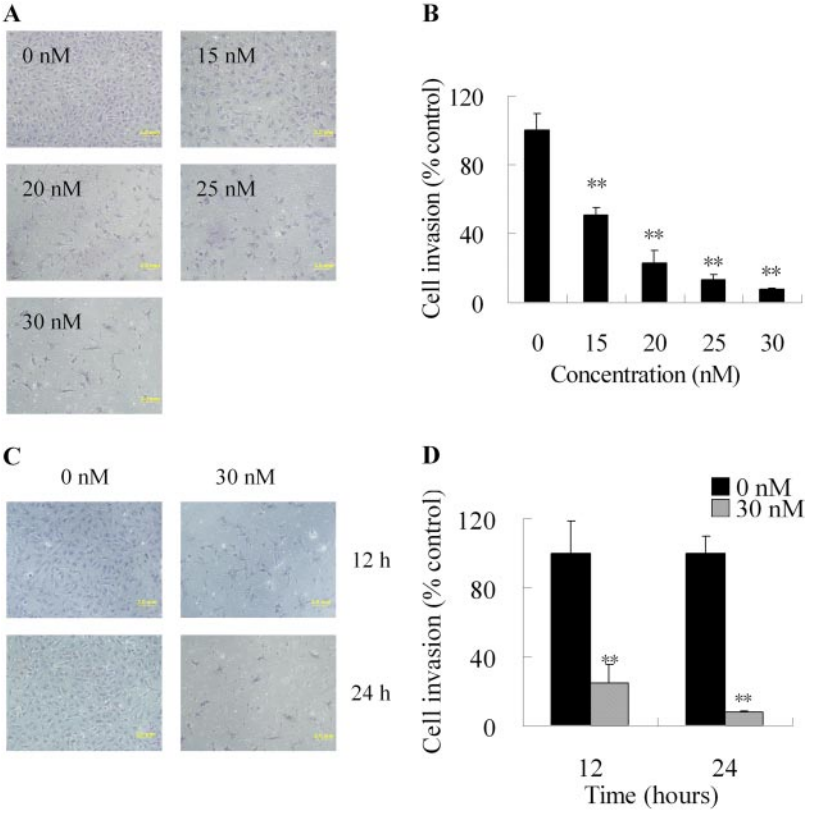

Fig. 3. Triptolide inhibited the invasion of TA-K cells. A and B, the concentration-dependent effect of triptolide on cell invasion. TA-K cells were pretreated with 0, 15, 20, 25, and 30 nM triptolide for 24 h. C and D, the time-dependent effect of triptolide on cell invasion. TA-K cells were pretreated with 30 nM triptolide for 12 and 24 h. The data are mean ± S.D. ($n = 3$). *, $p < 0.05$; **, $p < 0.01$ compared with the control.

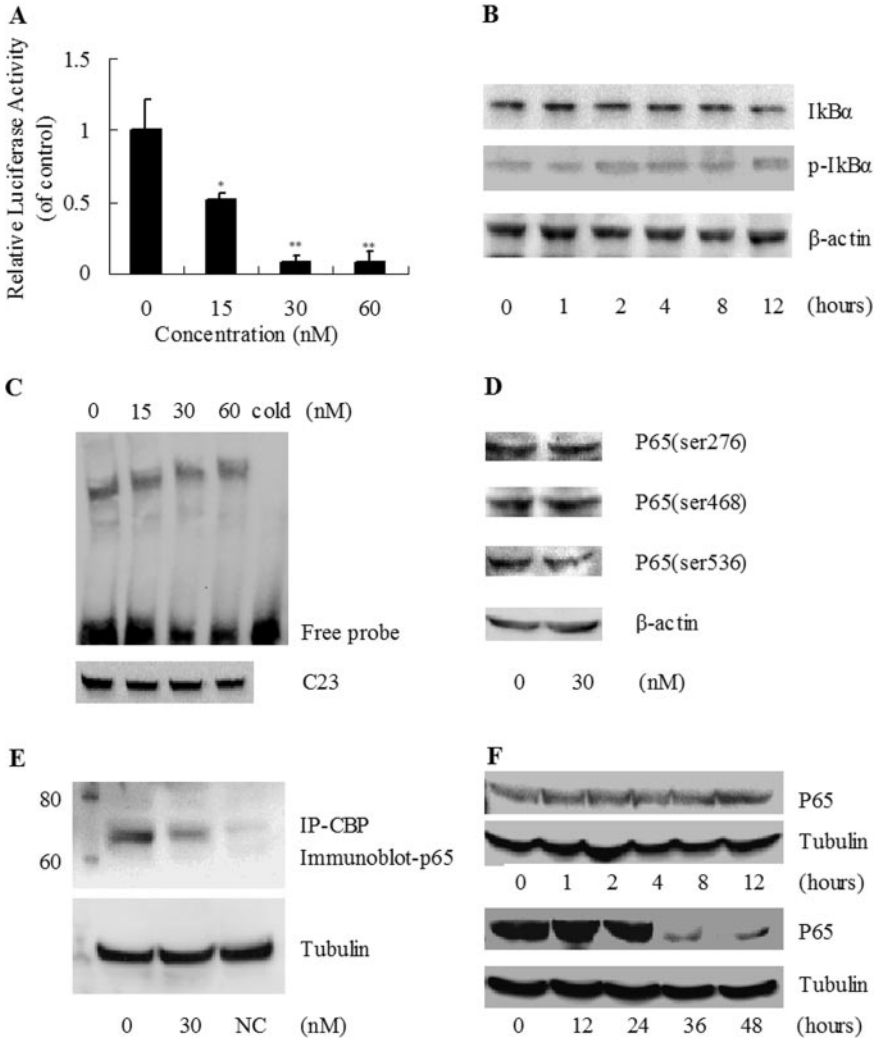

Fig. 4. Triptolide inhibited NF-κB transcriptional activity by down-regulating p65 expression and its association with CBP. A, relative luciferase activity of NF-κB. TA-K cells cotransfected with NF-κB and pGL-3 luciferase plasmid were treated with triptolide for 12 h. *, $p < 0.05$; **, $p < 0.01$ compared with the control. B, the total and phosphorylation level of IκBα. Cells were treated with 30 nM triptolide for 12 h followed by Western blotting. C, NF-κB binding activities. TA-K cells were treated with 0, 15, 30, and 60 nM triptolide for 12 h followed by electrophoretic mobility shift assay. D, the phosphorylation level of p65 in Ser276, Ser468, and Ser536 followed by Western blotting. Cells were treated with 30 nM triptolide for 12 h. E, the binding activities of CBP to p65. Cells treated with 30 nM triptolide for 12 h were immunoprecipitated with a CBP antibody followed by Western blot analysis with a p65 antibody (tubulin was used as loading control and nonspecific IgG was used as negative control). NC represents negative control. F, the effect of triptolide on p65 protein level. Cells were treated with 30 nM triptolide for indicated time followed by Western blotting.

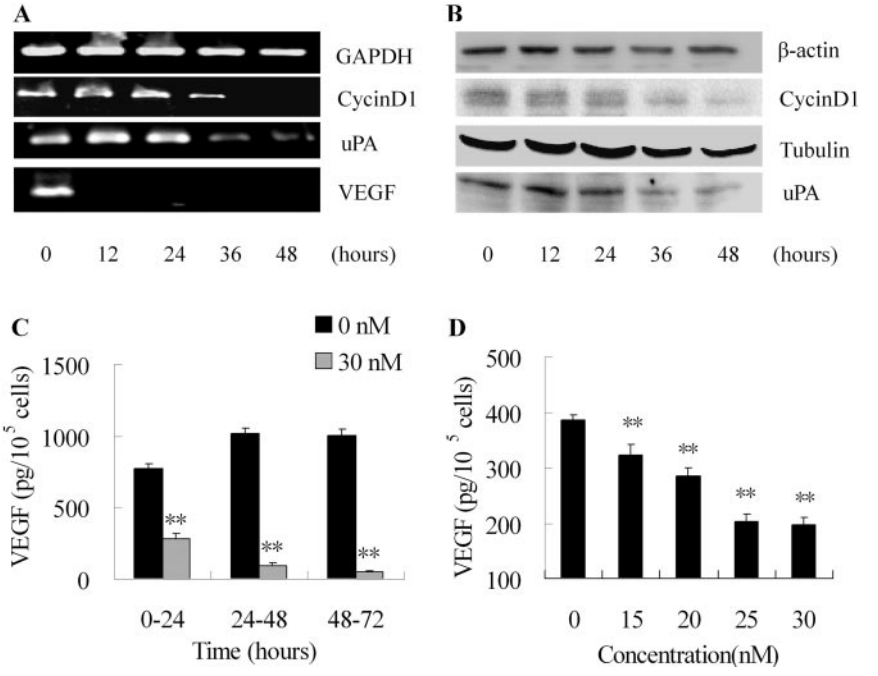

Fig. 5. Triptolide down-regulated NF-κB downstream gene expression in TA-K cells. A, the time-dependent effect of triptolide on cyclin D1, uPA, and VEGF mRNA levels. TA-K cells were treated with 30 nM triptolide for 0, 12, 24, 36, and 48 h. B, the time-dependent effect of triptolide on cyclin D1 and uPA protein levels. TA-K cells were treated with 30 nM triptolide for 0, 12, 24, 36, and 48 h. C and D, the time-dependent (C) and concentration effect (D) of triptolide on VEGF secretion. TA-K cells were treated with 30 nM triptolide for 24, 48, and 72 h and with 0, 15, 20, 25, and 30 nM for 12 h. The data are mean ± S.D. ($n = 3$). *, $p < 0.05$; **, $p < 0.01$ compared with the control.

VEGF, cyclin D1, and uPA. Taken together, triptolide functions as a NF-κB inhibitor with dual actions by disruption of p65/CBP interaction and by reduction of p65 protein.

The triptolide activity in inhibiting transcriptional activation but not DNA binding of NF-κB has been reported to be mediated through the C-terminal transactivation domains TA1 and TA2 of p65 (Lee et al., 1999; Qiu et al., 1999). We thus postulated that the triptolide effectiveness in our case may derive from their specific inhibition on TA1 and TA2 regions of p65. However, to examine whether the interrupted association of p65 to CBP/p300 was the result of direct effect on TA1 and TA2 domains of p65, further studies are required. More importantly, our data demonstrated that p65 knockdown significantly decreased VEGF production and invasive activity of TA-K cells (Supplemental Fig. 4). These data provide, at least in part, further mechanistic insights involving p65 into the antiangiogenic and anti-invasive mechanism of triptolide action.

The central role of the VEGF in pathologic angiogenesis and invasion, combined with its restricted expression in healthy adults, has spurred the development of a variety of therapeutic strategies aimed at blocking VEGF for antitumor therapy. The VEGF-specific antibody bevacizumab (Avastin) and receptor tyrosine kinase inhibitors are the best-known and well used antiangiogenic agents (Ferrara and Alitalo, 1999; Gerber, 2003). Bevacizumab has been the first-administered drug in clinic and has shown a promising effect in some metastatic cancers combined with other chemotherapy (Ranieri et al., 2006). However, being an antibody, bevacizumab has some characteristics that limit its efficacy, such as macromolecule, weak penetrability, and unsymmetrical distribution. In addition, phase III clinical trials demonstrated that multitargeted small-molecule receptor tyrosine kinase inhibitors possess a higher efficacy than specific anti-VEGF monotherapy, indicating the dominance of multitargeted small molecule in the clinical treatment (Jain et al., 2006). Here, our results showed that triptolide is a small molecule with multiple targets, including inhibiting cancer cell proliferation, tumor angiogenesis, and invasion.

Triptolide is such a small, soluble, stable, and multifunctional molecule that could be easily produced and conveniently delivered. In addition, use of this small molecule bypasses the vast majority of inconvenience and disadvantage associated with protein and gene therapy, such as poor permeability, immunogenicity, low efficacy, high cost, and so on. Third, triptolide has been used in clinic for the treatment of rheumatoid arthritis for decades, avoiding a long-term preclinical study. These merits further encourage the use of this small molecular compound in the chemoprevention and treatment of ATC.

The antiproliferative and proapoptotic activities of triptolide have been demonstrated in various tumor cell lines in vitro (Chang et al., 2001; Jiang et al., 2001; Lou and Jin, 2004) and in vivo models (Fidler et al., 2003; Yang et al., 2003; Phillips et al., 2007), which imply no tumor selectivity. In this study, we have identified novel antiangiogenesis and anti-invasion activities of triptolide in ATC cells through a mechanism that inhibits NF-κB transactivation. However, the inhibitory activity of triptolide on NF-κB transcriptional activation has been widely reported in large quantity of tumor cells as well as normal cells (Lee et al., 1999; Qiu et al., 1999; Jiang et al., 2001; Liu et al., 2007). Our data also showed that there exists no cell specificity of triptolide in inhibiting NF-κB activation in both TA-K and 8505C ATC cell lines. The above studies consequently lead to our hypothesis that triptolide, the angiogenesis and invasion inhibitor in ATC, may exert global antitumor activity through an universal inhibition of NF-κB transactivation. However, we

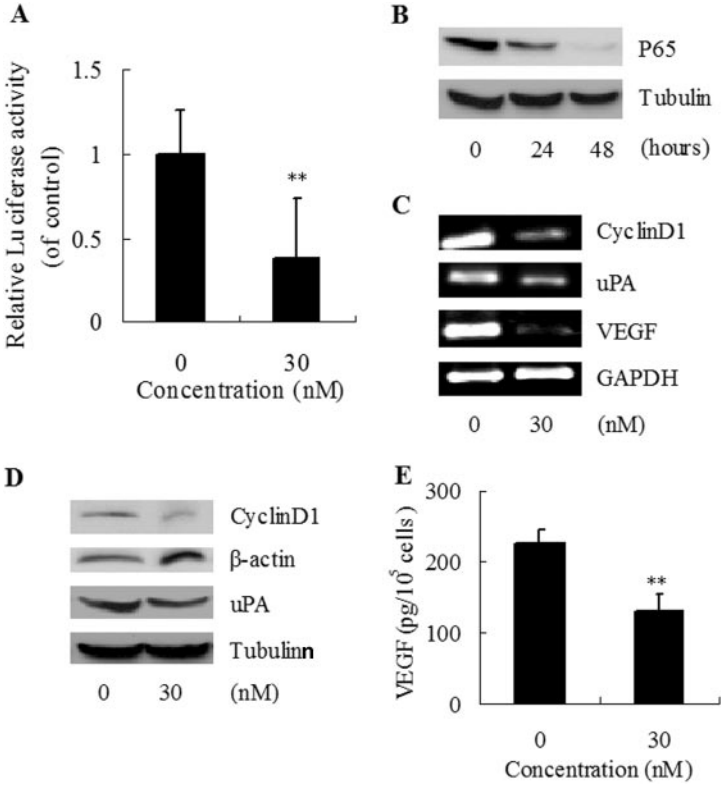

Fig. 6. Triptolide inhibited NF-κB transcriptional activity, p65 expression, and NF-κB downstream genes in 8505C cells. A, the relative luciferase activity of NF-κB. 8505C cells were treated with 30 nM triptolide for 12 h. B, the effect of triptolide on p65 protein level. 8505C cells were treated with 30 nM triptolide for 0, 24, and 48 h. C, the effect of triptolide on cyclin D1, uPA, and VEGF mRNA levels. 8505C cells were treated with 30 nM triptolide for 48 h. D, the effect of triptolide on cyclin D1 and uPA protein levels. 8505C cells were treated with 30 nM triptolide for 48 h. E, the effect of triptolide on VEGF secretion. 8505C cells were treated with 30 nM triptolide for 24 h. The data are mean ± S.D. ($n = 3$). *, $p < 0.05$; **, $p < 0.01$ compared with the control.

believe further studies in diverse cancer cells are warranted to conclusively clarify this important issue of triptolide on tumor selectivity.

In conclusion, we identify triptolide as a promising candidate agent for the treatment of patients with ATC and reveal its important model of action. Triptolide potently inhibits angiogenesis and invasion in ATC in part through targeting p65 subunit of NF-κB. This small molecule natural product may prove to be a much-needed candidate for the systemic therapy of ATC, which has a great prospect either used alone or in combination with conventional therapies. However, additional studies exploring the in vivo biological activity of triptolide are needed in further work and will potently support triptolide as a potential drug for human ATC.

Acknowledgments

We thank Dr. Hui Sun for kindly providing TA-K cells, Prof. Mingtao Li for the generous gift of pGL-3 vector, and Yijun Huang, Yuxi Zhou, Lijun Chen, Dong Xu, and Xingwen Su for their excellent technical assistance with this work.

References

Aggarwal BB (2004) Nuclear factor-kappaB: the enemy within. *Cancer Cell* **6:**203–208.

Baldwin AS Jr (1996) The NF-kappa B and I kappa B proteins: new discoveries and insights. *Annu Rev Immunol* **14:**649–683.

Carmeliet P and Jain RK (2000) Angiogenesis in cancer and other diseases. *Nature* **407:**249–257.

Chan EW, Cheng SC, Sin FW, and Xie Y (2001) Triptolide induced cytotoxic effects on human promyelocytic leukemia, T cell lymphoma and human hepatocellular carcinoma cell lines. *Toxicol Lett* **122:**81–87.

Chang WT, Kang JJ, Lee KY, Wei K, Anderson E, Gotmare S, Ross JA, and Rosen GD (2001) Triptolide and chemotherapy cooperate in tumor cell apoptosis. A role for the p53 pathway. *J Biol Chem* **276:**2221–2227.

Chen BJ (2001) Triptolide, a novel immunosuppressive and anti-inflammatory agent purified from a Chinese herb Tripterygium wilfordii Hook F. *Leuk Lymphoma* **42:**253–265.

Chilov D, Kukk E, Taira S, Jeltsch M, Kaukonen J, Palotie A, Joukov V, and Alitalo K (1997) Genomic organization of human and mouse genes for vascular endothelial growth factor C. *J Biol Chem* **272:**25176–25183.

Fang J, Zhou Q, Liu LZ, Xia C, Hu X, Shi X, and Jiang BH (2007) Apigenin inhibits tumor angiogenesis through decreasing HIF-1alpha and VEGF expression. *Carcinogenesis* **28:**858–864.

Ferrara N and Alitalo K (1999) Clinical applications of angiogenic growth factors and their inhibitors. *Nat Med* **5:**1359–1364.

Ferrara N, Gerber HP, and LeCouter J (2003) The biology of VEGF and its receptors. *Nat Med* **9:**669–676.

Ferrara N, Hillan KJ, and Novotny W (2005) Bevacizumab (Avastin), a humanized anti-VEGF monoclonal antibody for cancer therapy. *Biochem Biophys Res Commun* **333:**328–335.

Fidler JM, Li K, Chung C, Wei K, Ross JA, Gao M, and Rosen GD (2003) PG490–88, a derivative of triptolide, causes tumor regression and sensitizes tumors to chemotherapy. *Mol Cancer Ther* **2:**855–862.

Gerber HP (2003) Anti-angiogenesis: biology is the foundation for therapy. *Drug Discov Today* **8:**344–346.

Hicklin DJ and Ellis LM (2005) Role of the vascular endothelial growth factor pathway in tumor growth and angiogenesis. *J Clin Oncol* **23:**1011–1027.

Hoffmann A, Levchenko A, Scott ML, and Baltimore D (2002) The IkappaB-NF-kappaB signaling module: temporal control and selective gene activation. *Science* **298:**1241–1245.

Huang S, Pettaway CA, Uehara H, Bucana CD, and Fidler IJ (2001) Blockade of NF-kappaB activity in human prostate cancer cells is associated with suppression of angiogenesis, invasion, and metastasis. *Oncogene* **20:**4188–4197.

Huang S, Robinson JB, Deguzman A, Bucana CD, and Fidler IJ (2000) Blockade of nuclear factor-kappaB signaling inhibits angiogenesis and tumorigenicity of human ovarian cancer cells by suppressing expression of vascular endothelial growth factor and interleukin 8. *Cancer Res* **60:**5334–5339.

Jain RK, Duda DG, Clark JW, and Loeffler JS (2006) Lessons from phase III clinical trials on anti-VEGF therapy for cancer. *Nat Clin Pract Oncol* **3:**24–40.

Jiang XH, Wong BC, Lin MC, Zhu GH, Kung HF, Jiang SH, Yang D, and Lam SK (2001) Functional p53 is required for triptolide-induced apoptosis and AP-1 and nuclear factor-kappaB activation in gastric cancer cells. *Oncogene* **20:**8009–8018.

Karin M (2006) Nuclear factor-kappaB in cancer development and progression. *Nature* **441:**431–436.

Kiviharju TM, Lecane PS, Sellers RG, and Peehl DM (2002) Antiproliferative and proapoptotic activities of triptolide (PG490), a natural product entering clinical trials, on primary cultures of human prostatic epithelial cells. *Clin Cancer Res* **8:**2666–2674.

Kong D, Li Y, Wang Z, Banerjee S, and Sarkar FH (2007) Inhibition of angiogenesis and invasion by 3,3′-diindolylmethane is mediated by the nuclear factor-kappaB downstream target genes MMP-9 and uPA that regulated bioavailability of vascular endothelial growth factor in prostate cancer. *Cancer Res* **67:**3310–3319.

Lee KY, Chang W, Qiu D, Kao PN, and Rosen GD (1999) PG490 (triptolide) cooperates with tumor necrosis factor-alpha to induce apoptosis in tumor cells. *J Biol Chem* **274:**13451–13455.

Liu Q, Chen T, Chen G, Shu X, Sun A, Ma P, Lu L, and Cao X (2007) Triptolide impairs dendritic cell migration by inhibiting CCR7 and COX-2 expression through PI3-K/Akt and NF-kappaB pathways. *Mol Immunol* **44:**2686–2696.

Lou YJ and Jin J (2004) Triptolide down-regulates bcr-abl expression and induces apoptosis in chronic myelogenous leukemia cells. *Leuk Lymphoma* **45:**373–376.

Mareel M and Leroy A (2003) Clinical, cellular, and molecular aspects of cancer invasion. *Physiol Rev* **83:**337–376.

Mattioli I, Geng H, Sebald A, Hodel M, Bucher C, Kracht M, and Schmitz ML (2006) Inducible phosphorylation of NF-kappa B p65 at serine 468 by T cell costimulation is mediated by IKK epsilon. *J Biol Chem* **281:**6175–6183.

McIver B, Hay ID, Giuffrida DF, Dvorak CE, Grant CS, Thompson GB, van Heerden JA, and Goellner JR (2001) Anaplastic thyroid carcinoma: a 50-year experience at a single institution. *Surgery* **130:**1028–1034.

Neff RL, Farrar WB, Kloos RT, and Burman KD (2008) Anaplastic thyroid cancer. *Endocrinol Metab Clin North Am* **37:**525–538.

Pasieka JL (2003) Anaplastic thyroid cancer. *Curr Opin Oncol* **15:**78–83.

Phillips PA, Dudeja V, McCarroll JA, Borja-Cacho D, Dawra RK, Grizzle WE, Vickers SM, and Saluja AK (2007) Triptolide induces pancreatic cancer cell death via inhibition of heat shock protein 70. *Cancer Res* **67:**9407–9416.

Prewett M, Huber J, Li Y, Santiago A, O'Connor W, King K, Overholser J, Hooper A, Pytowski B, Witte L, et al. (1999) Antivascular endothelial growth factor receptor (fetal liver kinase 1) monoclonal antibody inhibits tumor angiogenesis and growth of several mouse and human tumors. *Cancer Res* **59:**5209–5218.

Qiu D, Zhao G, Aoki Y, Shi L, Uyei A, Nazarian S, Ng JC, and Kao PN (1999) Immunosuppressant PG490 (triptolide) inhibits T-cell interleukin-2 expression at the level of purine-box/nuclear factor of activated T-cells and NF-kappaB transcriptional activation. *J Biol Chem* **274:**13443–13450.

Ranieri G, Patruno R, Ruggieri E, Montemurro S, Valerio P, and Ribatti D (2006) Vascular endothelial growth factor (VEGF) as a target of bevacizumab in cancer: from the biology to the clinic. *Curr Med Chem* **13:**1845–1857.

Schmitt M, Horbach A, Kubitz R, Frilling A, and Häussinger D (2004) Disruption of hepatocellular tight junctions by vascular endothelial growth factor (VEGF): a novel mechanism for tumor invasion. *J Hepatol* **41:**274–283.

Tan RK, Finley RK 3rd, Driscoll D, Bakamjian V, Hicks WL Jr, and Shedd DP (1995) Anaplastic carcinoma of the thyroid: a 24-year experience. *Head Neck* **17:**41–48.

Weis S, Cui J, Barnes L, and Cheresh D (2004) Endothelial barrier disruption by VEGF-mediated Src activity potentiates tumor cell extravasation and metastasis. *J Cell Biol* **167:**223–229.

Yang S, Chen J, Guo Z, Xu XM, Wang L, Pei XF, Yang J, Underhill CB, and Zhang L (2003) Triptolide inhibits the growth and metastasis of solid tumors. *Mol Cancer Ther* **2:**65–72.

Zhong H, May MJ, Jimi E, and Ghosh S (2002) The phosphorylation status of nuclear NF-kappa B determines its association with CBP/p300 or HDAC-1. *Mol Cell* **9:**625–636.

Zhong H, Voll RE, and Ghosh S (1998) Phosphorylation of NF-kappa B p65 by PKA stimulates transcriptional activity by promoting a novel bivalent interaction with the coactivator CBP/p300. *Mol Cell* **1:**661–671.

Address correspondence to: Guangmei Yan, Department of Pharmacology, Zhong-shan Medical College, Sun Yat-Sen University, 74 Zhongshan Road II, Guangzhou, 510089, P.R. China. E-mail: ygm@mail.sysu.edu.cn